# Polaron Absorption in a Perovskite Manganite $La_{0.7}Ca_{0.3}MnO_3$

K. H. Kim, J. H. Jung, and T. W. Noh*

*Department of Physics, Seoul National University, Seoul 151-742, Korea*

(Received 30 September 1997)

Temperature dependent optical conductivity spectra of a $La_{0.7}Ca_{0.3}MnO_3$ (LCMO) sample were measured. In the metallic regime at very low temperatures, they clearly showed two types of absorption features, i.e., a sharp Drude peak and a broad midinfrared absorption band, which could be explained as coherent and incoherent bands of a large lattice polaron. Electrodynamic analyses suggest that the elementary excitation in LCMO should be in a strong coupling regime and have interactions with the spin degree of freedom. [S0031-9007(98)06851-3]

PACS numbers: 78.20.Ci, 72.15.Gd, 75.30.Kz, 75.50.Cc

The recent discovery of colossal magnetoresistance phenomena in doped perovskite manganites, $La_{1-x}A_xMnO_3$ ($A = Sr, Ca$) has generated considerable interest. For doping concentrations with $0.2 \lesssim x \lesssim 0.5$, the materials show a transition from a paramagnetic insulator to a ferromagnetic metal upon cooling near the Curie temperature $T_C$. The correlation between metallicity and ferromagnetism has been explained by the double exchange (DE) model which is based on the strong Hund coupling between $t_{2g}$ and $e_g$ electrons [1,2].

In addition to the coupling between charge and spin degrees of freedom, many theoretical [3,4] and experimental [5–9] papers have shown that a coupling between charge and lattice degrees of freedom is quite significant. Especially, giant oxygen isotope shifts of $T_C$ in $(La, Ca)MnO_3$ compounds have indicated that the electron-phonon coupling is very large for the Ca-doped manganites [10]. Therefore, it is widely accepted that a polaron plays an important role near and above $T_C$ in the manganites.

Some experimental papers demonstrated that local lattice distortions exist even in the metallic phase [7,11]. Recently, we observed that the internal phonon modes of $La_{0.7}Ca_{0.3}MnO_3$ (LCMO) showed significant frequency shifts, which were explained in terms of changes in electronic screening during a crossover from a localized polaron regime above $T_C$ to a delocalized one below $T_C$. For the low temperature ($T$) state, there are numerous theoretical predictions based on a large polaron coherent motion [4], a small polaron tunneling [12], and a formation of orbital liquid states [13]. However, at this moment, the exact nature of the low-$T$ metallic state is not clearly understood.

In this Letter, we will address polaron absorption features, especially a very unusual polaron state at low $T$, in LCMO. Detailed characteristics of the polaron absorption at low $T$ could be explained in terms of the large lattice polaron picture by Emin [14]. Moreover, an electrodynamic analysis revealed that *the large polaron in LCMO should be in a strong coupling regime,* as far as we know, which has not been realized in other physical systems before.

A polycrystalline LCMO sample was prepared by a standard solid-state reaction method [15]. Near normal incidence reflectivity spectra, $R(\omega)$, were measured between 8 meV and 30 eV. A Fourier transform spectrophotometer was used for 8 meV–2.5 eV and a grating type monochromator was used between 0.4 and 7.0 eV. Above 6.0 eV, the synchrotron radiation source from the Normal Incidence Monochromator beam line at Pohang Light Source (PLS) was used [16]. To measure $T$-dependent $R(\omega)$ below 2.5 eV, a liquid He-cooled cryostat was used.

Optical conductivity spectra, $\sigma(\omega)$, were obtained using the Kramers-Kronig transformation. For this analysis, $R(\omega)$ below 8 meV were extrapolated with the Hagen-Rubens relation [17]. For a high frequency region, reflectivity, $R$, at 30 eV was extended up to 40 eV, above which $\omega^{-4}$ dependence was assumed. We found that there were less than 2.0% changes of $R$ with $T$ in a frequency region between 2.0 and 2.5 eV, so we attached low temperature $R$ data below 2.5 eV smoothly with room temperature data above it. The errors due to such an extrapolation were estimated to be about 10% in $\sigma(\omega)$ around 2.5 eV and smaller below 2.0 eV.

Figure 1(a) shows that there are significant spectral weight (SW) transfers from high to low energies with decreasing $T$. A crossover energy is about 0.5 eV. It is noted that the spectra below 0.5 eV, shown in Fig. 1(b), can be characterized by two types of responses, i.e., a sharp Drude peak in a far-infrared (far-IR) region and a broad absorption band in a mid-IR region. So, a corresponding conductivity spectrum can be written as a sum of the two contributions: $\sigma(\omega) = \sigma_{\mathrm{Drude}}(\omega) + \sigma_{\mathrm{MIR}}(\omega)$. A clearer picture on the development of the far-IR Drude peak is also shown in the inset of Fig. 1(b). As $T$ decreases, $\sigma_{\mathrm{MIR}}(\omega)$ increases initially but becomes saturated around 120 K. However, $\sigma_{\mathrm{Drude}}(\omega)$ increases continuously without any saturation. The behaviors of $\sigma(\omega)$ in LCMO are quite different from those in a $Nd_{0.7}Sr_{0.3}MnO_3$ film [9], which showed no Drude peak and a strong and quite symmetric mid-IR band. On the other hand, the general behaviors of $\sigma(\omega)$ in LCMO are somewhat similar to those in a $La_{0.7}Sr_{0.3}MnO_3$ single crystal [18]. However, for $La_{0.7}Sr_{0.3}MnO_3$, quantitative information of both $\sigma_{\mathrm{Drude}}(\omega)$ and $\sigma_{\mathrm{MIR}}(\omega)$ was still lacking, and the origin of the mid-IR band has not been clearly explained yet [18].

  

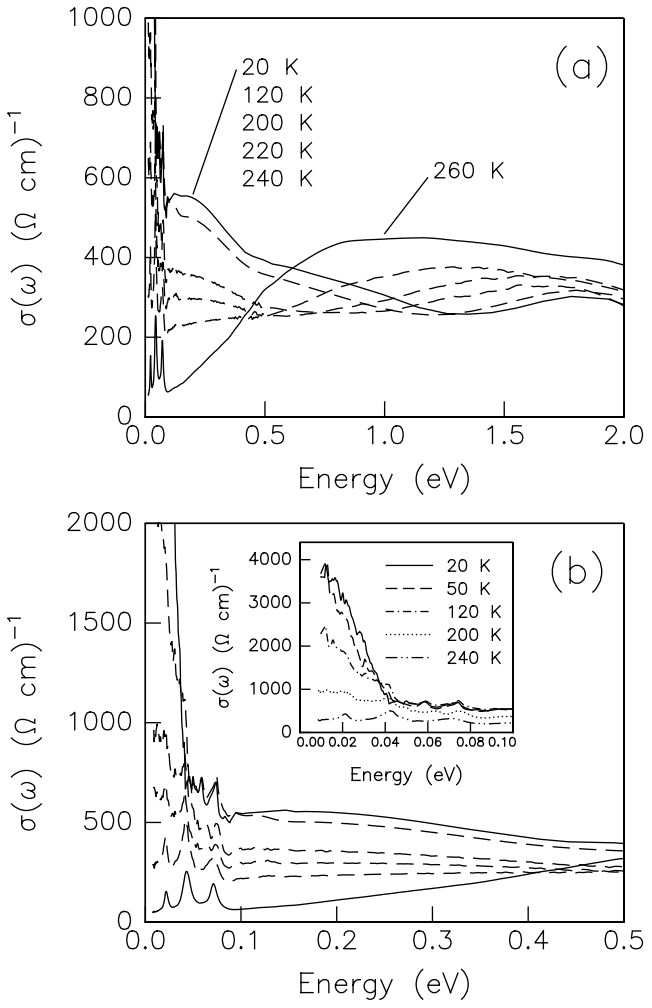


FIG. 1. (a) Optical conductivity spectra below 2 eV. (b) Optical conductivity spectra below 0.5 eV. Temperature ranges are the same as those in (a). Inset shows detailed optical conductivity spectra in a far-IR region.

Above $T_C$, i.e., in the insulating regime, it is widely accepted that a small polaron, called the "Holstein polaron," plays an important role. In addition, $\sigma_{\mathrm{MIR}}(\omega)$ below 0.8 eV at 260 K can be fitted reasonably well with the small polaron model [19,20], just like the case of $(\mathrm{La,Sr})_2\mathrm{NiO}_{4+\delta}$ [21]. However, below $T_C$, it is not known clearly whether a large polaron coherent motion [4] or a small polaron tunneling [12] will be the origin of the metallic behavior in LCMO.

Emin investigated frequency responses of large and small polaron absorption [14]. A coherent band of the large polaron should show up only at lower frequencies below characteristic phonon modes and become more significant as $T$ decreases. In addition, its photoionization should bring out an incoherent mid-IR band which is very asymmetric and shows a long tail above its peak position. On the other hand, a coherent band of the small polaron, i.e., polaron tunneling band, should occur at an energy region much lower than the characteristic phonon modes. Behaviors of both $\sigma_{\mathrm{Drude}}(\omega)$ and $\sigma_{\mathrm{MIR}}(\omega)$ at $T \lesssim 120$ K, shown in Fig. 1, are quite consistent with the large polaron absorption features, predicted by Emin. As shown in the inset, the Drude peak becomes evident below the bending phonon mode frequency, i.e., $\sim 330\ \mathrm{cm}^{-1}$, and its width does not change too much. Moreover, $\sigma_{\mathrm{MIR}}(\omega)$ near 20 K is quite asymmetric and shows a long tail above its peak position. From this observation, $\sigma_{\mathrm{Drude}}(\omega)$ at $T \lesssim 120$ K can be attributed to a coherent motion of a large polaron, and $\sigma_{\mathrm{MIR}}(\omega)$ can be attributed to its incoherent absorption band [22].

To get quantitative information on electrodynamic responses of the large polaron in LCMO, we looked into the real part of its dielectric function, $\varepsilon_1$. Figure 2 shows $T$-dependent $\varepsilon_1$ spectra. At a low frequency $\varepsilon_1$ becomes negative, indicating that LCMO is in a metallic state. In the Drude model, the complex dielectric function $\tilde{\varepsilon}(\omega)$ can be written as

$$\tilde{\varepsilon}(\omega) = \varepsilon_\infty - \frac{\omega_p^2}{\omega^2 + i\omega/\tau}, \tag{1}$$

where $\omega_p$ and $\tau$ are a bare plasma frequency and a relaxation time of free carriers, respectively. In addition, $\varepsilon_\infty$ is the dielectric constant at a high frequency. If $\omega \gg 1/\tau$, $\tilde{\varepsilon}(\omega) \approx \varepsilon_\infty - \omega_p^2/\omega^2$. In a real metallic sample, however, mid-IR and interband absorptions also contribute to $\tilde{\varepsilon}(\omega)$. If their contributions to $\tilde{\varepsilon}(\omega)$ vary slowly in $\omega$, $\varepsilon_1$ can be approximated as $\varepsilon_h - \omega_p^2/\omega^2$, where $\varepsilon_h$ represents a "background" dielectric constant at a high frequency determined by $\varepsilon_\infty$ and contributions from the interband and the mid-IR absorptions. Then, the slope in a $\varepsilon_1$ vs $\omega^{-2}$ plot will provide the value of $\omega_p^2$ for the coherent band. The inset of Fig. 2 shows the $\varepsilon_1$ vs $\omega^{-2}$ plot. ($\varepsilon_h$ was estimated to be about 4.9.) The solid and

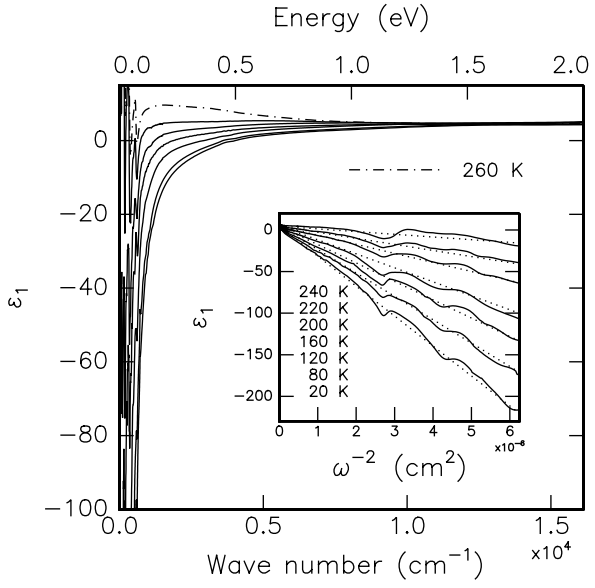


FIG. 2. The real part of the complex dielectric function, $\varepsilon_1$, spectra. Inset shows the $\varepsilon_1$ vs $\omega^{-2}$ plots at various temperatures. Temperature ranges are the same with those shown in the inset except 260 K.

dotted lines are experimental data and linear guidelines, respectively. Except phonon frequency regions, the $\varepsilon_1$ vs $\omega^{-2}$ plots are quite linear.

The experimental values of $\omega_p^2$ are plotted in Fig. 3(a). Interestingly, $\omega_p^2$ is approximately proportional to $(T_C - T)$. The increase of $\omega_p^2$ upon cooling is in good agreement with photoemission data which showed that the density of states at the Fermi energy increased progressively below $T_C$ [23]. Note that $\omega_p^2 = 4\pi ne^2/m^*$, where $n$ and $m^*$ represent a density and an effective mass of the free carriers, respectively. In the large lattice polaron picture, $m^* = m_b + M_p$, where $m_b$ is the band mass of the carriers and $M_p$ represents the atomic contribution due to the shift of the equilibrium position of each atom when the polaron moves by a lattice constant [14,24].

To get a further insight on the coherent polaron motion in LCMO, we need information on its dc resistivity, $\rho$. Since the $\rho$ data for a LCMO single crystal were not available, they were estimated from the $R$ data using the Hagen-Rubens relation [17,25]. As shown in Fig. 3(b), $\rho$ increases rapidly above 150 K. Using a relation such that $\rho = m^*/ne^2\tau$, the scattering rate $1/\tau$ for the Drude peak was estimated and plotted in Fig. 3(c). Another interesting physical quantity is its mean free path, $l$ $[= \tau\hbar(3\pi^2 n)^{1/3}/m^*]$. If we assume that $n$ is equal to 0.3 hole per Mn at 20 K, the $\omega_p^2$ value predicts $m^*$ as $13m_e$. Using the experimental values of $\tau$, $l$ could be estimated. At 20 K, $l \sim 25$ Å which is much larger than the lattice constant of about 3.9 Å. However, as $T$ increases, $l$ becomes smaller and approaches the lattice constant value near $T_C$: $l \sim 4.2$ Å at 240 K. Note that this result is consistent with the Ioffe-Regel criterion for metal-insulator transitions; i.e., $l \sim$ lattice constant [26].

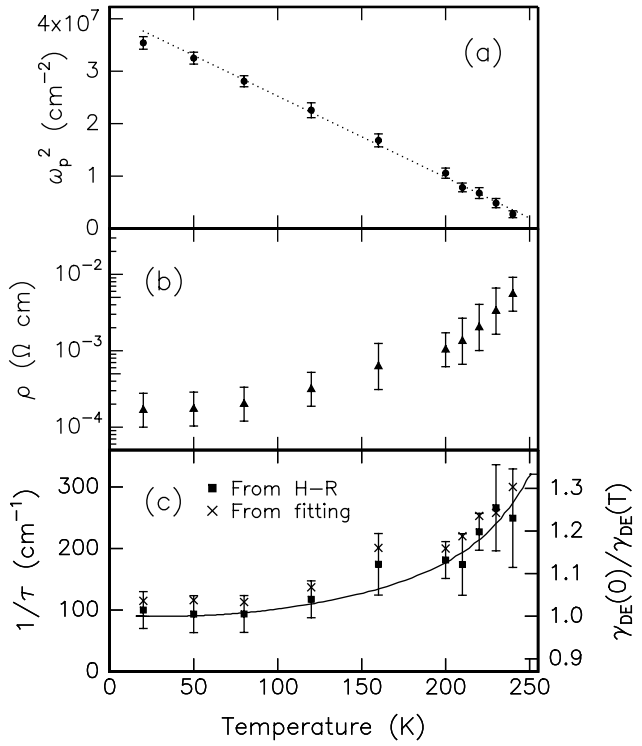


FIG. 3. (a) Values of $\omega_p^2$ determined from the $\varepsilon_1$ vs $\omega^{-2}$ plots. The dotted line is a linear guide for the eye. (b) Resistivity values determined from the Hagen-Rubens relation. (c) Scattering rates of the free carriers (solid squares) determined from (a) and (b). For checking the internal consistency of our analysis, the scattering rates (crosses) were also estimated using other methods, i.e., fitting the far-IR $\sigma(\omega)$. The behavior of $1/\gamma_{\mathrm{DE}}(T)$ is overlapped as a solid line.

The solid squares and the solid circles in Fig. 4 represent spectral weights of the Drude peak and the mid-IR band, respectively. (The open diamonds represent the total SW.) The Drude weight (DW) of the coherent polaron motion was evaluated using $(2m_e/\pi e^2 N)(\omega_p^2/8)$, where $m_e$ is an electron mass and $N$ is the number of Mn atoms per unit volume. Then, the total effective carrier number below a cutoff energy, $N_{\mathrm{eff}}(\omega_c)$, can be estimated from

$$N_{\mathrm{eff}}(\omega_c) = \frac{2m_e}{\pi e^2 N}\int_0^{\omega_c}\sigma(\omega)\,d\omega\,. \qquad (2)$$

We chose the cutoff energy $\hbar\omega_c$ as 0.5 eV. By subtracting the DW from $N_{\mathrm{eff}}(\omega_c)$, the spectral weight of the mid-IR band (SWMB) was obtained. As $T$ decreases, the SWMB increases but saturates at low temperatures. On the other hand, the DW can be scaled with $(T_C - T)$ reasonably well. The DW comprises a small portion of $N_{\mathrm{eff}}(\omega_c)$ below $T_C$: at 240 K, DW $\approx 0.07N_{\mathrm{eff}}(\omega_c)$ and even at 20 K, DW $\approx 0.33N_{\mathrm{eff}}(\omega_c)$. The values of the DW are very small at overall temperatures, compared with the doped carrier density, i.e., 0.3 hole per Mn. The small values of the DW might come from the large effective mass of the coherent polaron motion, especially at low $T$. In the case of a strongly coupled large polaron, $M_p \approx 0.02m_b\alpha^4$, where $\alpha$ represents the Fröhlich coupling constant [24]. If we assume $m_b = m_e$, $\alpha$ is estimated to be about 5, which suggests that the large polaron in LCMO remains in a

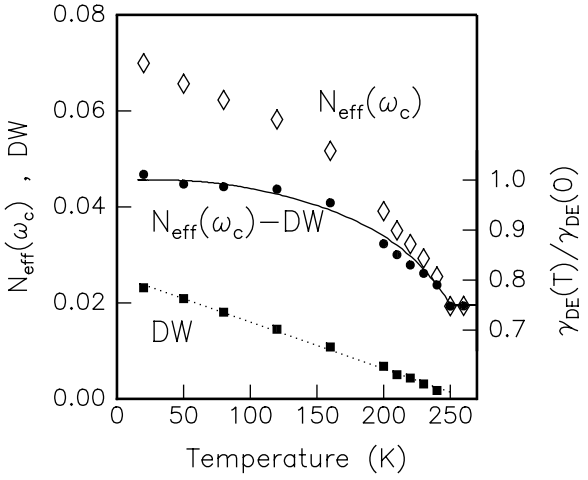


FIG. 4. $T$ dependence of $N_{\mathrm{eff}}$ (0.5 eV) (open diamonds), Drude weight (solid squares), and spectral weight of the mid-IR band (solid circles) in $La_{0.7}Ca_{0.3}MnO_3$. A solid line represents the behavior of $\gamma_{\mathrm{DE}}(T)$. A dotted line is a linear guide.

strong coupling regime. The size of the large polaron was estimated to be $(3/\alpha)[\pi\hbar/(4m_e\omega_0)]^{1/2} \approx 7$ Å, which is in agreement with the theoretical work by Röder *et al.* [4]. (The characteristic phonon frequency $\omega_0$ was chosen to be 300 $cm^{-1}$.)

In the literature, a realization of the strongly coupled large polaron was questioned due to its screening effect arising from dense carrier concentrations [20]. In $La_{0.7}Ca_{0.3}MnO_3$, there are lots of $Mn^{3+}$ sites which are susceptible to the local Jahn-Teller distortion, so the screening effect could be very important. However, in the DE model, a motion of a carrier at the metallic regime can be affected by spin ordering [27]. Therefore, the lattice at low $T$ can be also influenced by the long range spin ordering [6]. Under this influence, the coupling between the electron and the lattice in LCMO could be extended beyond a single lattice site. A recent pulsed neutron diffraction study also shows that the lattice polaron becomes more extended at low $T$ [11].

Our experimental data also clearly indicate that *the lattice polaron state in LCMO is also coupled with the spin degree of freedom.* According to the large lattice polaron theory by Emin [14], $1/\tau$ should be linearly proportional to $T$. Figure 3(c) shows that $1/\tau$ for the coherent polaron band remains nearly constant below 120 K and starts to increase above 160 K. In the DE picture, as $T$ approaches $T_C$, the free carriers are more likely to be scattered by the spin fluctuation. In the mean field limit, such a spin alignment effect could be represented by $\gamma_{\mathrm{DE}}(T) \equiv \langle\cos(\theta/2)\rangle$, which is a thermodynamic average of $\cos(\theta/2)$, where $\theta$ is an angle between nearest neighbor spins [2]. Shown as a solid line in Fig. 3(c), $1/\tau$ can be approximately scaled with $1/\gamma_{\mathrm{DE}}(T)$. Moreover, it is very interesting to see that the $T$ dependence of the SWMB is close to $\gamma_{\mathrm{DE}}(T)$, shown as the solid line in Fig. 4. Therefore, it is highly likely that both the coherent and the incoherent polaron bands are related to the spin degree of freedom. Note that a similar coupling existed in the phonon frequency renormalization [5] through $\tilde{\omega}_q \simeq \omega_q[1 - \beta/\gamma_{\mathrm{DE}}(T)]^{1/2}$.

In summary, we investigated the optical responses of a perovskite manganite $La_{0.7}Ca_{0.3}MnO_3$. They showed a Drude peak and a broad midinfrared absorption band. At low temperatures, these absorption features were interpreted as coherent and incoherent bands of a large lattice polaron. The electrodynamic analysis suggested that the polaron might be in a strong coupling regime, which is quite unique in this manganite. Moreover, the coherent and incoherent bands seem to have strong correlations with the spin degree of freedom.

We thank E. J. Choi, Jaejun Yu, B. I. Min, and H. Y. Choi for useful discussions. This work was financially supported by the Ministry of Education through the Basic Science Research Institute program BSRI-97-2416, and by KOSEF through Grant No. 96-0702-02-01-3 and the RCDAMP at Pusan National University. Experiments at PLS were supported by MOST and POSCO.

*Also at LG CIT, Seoul 137-742, Korea.

[1] C. Zener, Phys. Rev. **82**, 403 (1951); P. W. Anderson and H. Hasegawa, *ibid.* **100**, 675 (1955); P. G. de Gennes, *ibid.* **118**, 141 (1960).
[2] K. Kubo and N. Ohata, J. Phys. Soc. Jpn. **33**, 21 (1972).
[3] A. J. Millis, P. B. Littlewood, and B. I. Shraiman, Phys. Rev. Lett. **77**, 175 (1996); A. J. Millis, Phys. Rev. B **54**, 5405 (1996).
[4] H. Röder, J. Zhang, and A. R. Bishop, Phys. Rev. Lett. **76**, 1356 (1996).
[5] K. H. Kim *et al.*, Phys. Rev. Lett. **77**, 1877 (1996).
[6] J. M. De Teresa *et al.*, Nature (London) **386**, 256 (1997); M. R. Ibarra *et al.*, Phys. Rev. Lett. **75**, 3541 (1995).
[7] S. J. L. Billinge *et al.*, Phys. Rev. Lett. **77**, 715 (1996).
[8] M. Jaime *et al.*, Phys. Rev. Lett. **78**, 951 (1997).
[9] S. G. Kaplan *et al.*, Phys. Rev. Lett. **77**, 2081 (1996).
[10] G. Zhao *et al.*, Nature (London) **381**, 676 (1996).
[11] D. Louca *et al.*, Phys. Rev. B **56**, R8475 (1997); for a related work, see also J.-S. Zhou *et al.*, Phys. Rev. Lett. **79**, 3234 (1997).
[12] J. D. Lee and B. I. Min, Phys. Rev. B **55**, 12 454 (1997).
[13] S. Ishihara, M. Yamanaka, and N. Nagaosa, Phys. Rev. B **56**, 686 (1997).
[14] D. Emin, Phys. Rev. B **48**, 13 691 (1993), and references therein.
[15] Structure of LCMO is pseudocubic with very small orthorhombic distortions at overall temperatures. Therefore, anisotropy effects on the spectral response as well as transport can be neglected. See P. G. Radaelli *et al.*, Phys. Rev. B **56**, 8265 (1997).
[16] J. H. Jung *et al.*, Phys. Rev. B **55**, 15 489 (1997).
[17] K. H. Kim *et al.*, Phys. Rev. B **55**, 4023 (1997).
[18] Y. Okimoto *et al.*, Phys. Rev. Lett. **75**, 109 (1995); Y. Okimoto *et al.*, Phys. Rev. B **55**, 4206 (1997).
[19] R. Mühlstroh and H. G. Reik, Phys. Rev. **162**, 703 (1967).
[20] A. S. Alexandrov and N. F. Mott, *Polarons and Bipolarons* (World Scientific, Singapore, 1995), Chaps. 1 and 8.
[21] X.-X. Bi and P. C. Eklund, Phys. Rev. Lett. **70**, 2625 (1993).
[22] This assignment of the large polaron is in good agreement with the neutron pair distribution function study [7]. However, the work also showed that local lattice distortions, indicating small polaron states, can exist well below $T_C$ down to ~160 K. Therefore, in the crossover regime, some carriers might remain in a small polaron state.
[23] J.-H. Park *et al.*, Phys. Rev. Lett. **76**, 4215 (1996).
[24] G. D. Mahan, *Many-Particle Physics* (Plenum, New York, 1990), Chaps. 4 and 6.
[25] Sum rule analyses by $2\pi^2/\rho = \int_0^\infty [\varepsilon_\infty - \varepsilon(\omega)]\, d\omega$ gave nearly the same values of $\rho$ below 200 K. Refer to *Handbook of Optical Properties of Solids*, edited by E. D. Palik (Academic Press, New York, 1985), Chap. 3.
[26] *The Metallic and Nonmetallic States of Matter*, edited by P. P. Edwards and C. N. R. Rao (Taylor & Francis, London, 1985), Chap. 1.
[27] Neglecting the lattice distortion effects, such a coupling between electron and spin degrees of freedom can result in an elementary excitation, called a "spin polaron."